ACTIVE CONTROL OF THE FIELD DIFFRACTED BY THE REFLECTING WALL OF A SEMI-ANECHOIC ROOM

Cédric Pinhède[1] **Dominique Habault**[1] **Emmanuel Friot**[2]
Philippe Herzog[3]
[1] LMA - CNRS, 4 impasse Nikola Tesla, 13013 Marseille, France
[2] CNRS, 13 Bd Rabatau, 13008 Marseille, France
[3] ARTEAC-LAB SAS, 8 allée Léon Gambetta, Place de l'innovation (CIC), 13001 Marseille, France
pinhede@lma.cnrs-mrs.fr

ABSTRACT

The use of an anechoic room for characterizing low frequency loudspeakers is a classical solution but it is not sufficient especially below the cut-off frequency of the room. The goal of the present study is to combine passive and active reduction techniques in order to control the field diffracted by the walls at low frequencies using active techniques. As a first full-scale test this study is dedicated to the experimental validation of an active control method used to reproduce, in a semi-anechoic room, free field conditions, that is without reflections from the walls. The main point is that the diffracted pressure cannot be directly measured. A strategy is developed to obtain this pressure from measurements of total pressure on a surface surrounding the source to be characterized. Active control techniques are then used to drive an array of actuators to minimize the estimated diffracted field. Therefore the active control method includes two steps. The first one, off-line, consists in identifying an approximation of the operator which relates the diffracted pressure to the measured total pressures. The second one is the control of the estimated diffracted pressure.

1. INTRODUCTION

An accurate characterization of an acoustic source requires free field conditions. To obtain these conditions many techniques are used like passive resonators, active absorbents [1–3], Field separation Method (FSM) [4, 5] or others [6]. A classical choice is to use an anechoic room [7]. However the thickness of the lining limits the anechoicity at lower frequencies because of the sound reflection due to the walls.
Our long-term project is to realize a hybrid passive/active anechoic room by combining passive absorbing material with an active control technique [8–12].
An anechoic room aims at minimizing the pressure diffracted by the walls and the main difficulty is that this diffracted pressure cannot be directly measured. Here the strategy is based on the use of an operator which links the diffracted pressure to the total pressures measured on an array of microphones. Some works in 3D were previously developed [13–16]. The test-case presented here is a semi-anechoic room with control of the pressure diffracted by the rigid wall over the frequency range $40 - 200$ Hz, see Fig. 1.
The method involves two steps. The first one is to estimate the diffracted pressure using an array of microphones located near the reflecting wall and the second one is to cancel this pressure by control sources fixed on the wall.

2. THEORY

An approach for active anechoicity [10] consists in cancelling the pressure diffracted by the walls when a primary source is being measured inside a room. Here for practical reasons it was chosen to apply this approach to a semi-anechoic room although this case does not follow the theoretical assumptions of [10]. The example is illustrated by Fig. 1, where a source S is characterized from a pressure measurements at a point M in the semi-anechoic room. The goal is therefore to minimize the diffracted pressure at point M in order to measure only the incident pressure radiated by the source.

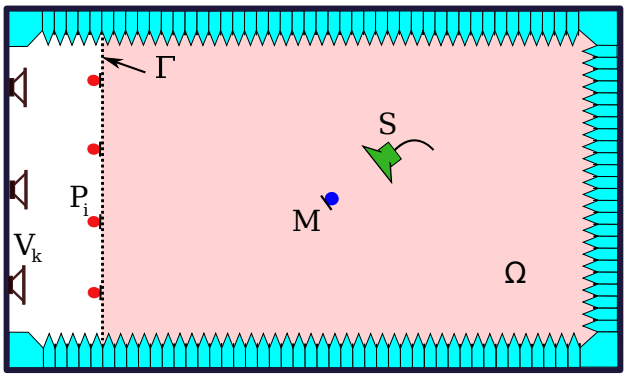

Figure 1. The geometry of the problem

The method for active control of the diffracted pressure is split in two steps. First, the identification of the diffracted pressure is carried out with an array P_Γ of N^Γ microphones P_i located on the surface Γ, named "identification microphones". Second, the active control drives an array of N^C control sources V_k located on the wall.

The main difficulty lies in the cancellation of the diffracted pressure which cannot be directly measured. As shown in reference [10], an operator $\mathcal{H}$ can be used to relate the diffracted pressure at a point M inside the volume Ω to the total pressures measured at points P_Γ. For a source S inside the volume Ω, the diffracted pressure at M, for each frequency, can be written as :

$$p_{dif}(S,M) \simeq \sum_{i=1}^{N^\Gamma} p_{tot}(S,P_i)\mathcal{H}(P_i,M) \qquad (1)$$

where p_{tot} is the total pressure measured at microphones P_i.

The identification of the operator $\mathcal{H}$ is based on the use of a reference source $\tilde{S}$ whose radiation pattern is known. The method is briefly exposed here, more details can be found in [10].

As the operator $\mathcal{H}$ does not depend on the source, it can be obtained by minimizing a linear system Eqn. (2) for a set of N^H positions - inside the volume Ω - of the reference source $\tilde{S}$:

$$F(\tilde{S},M) = \sum_{j=1}^{N^H} \left| \, p_{dif}(\tilde{S}_j,M) - \sum_{i=1}^{N^\Gamma} p_{tot}(\tilde{S}_j,P_i)\,\mathcal{H}(P_i,M) \, \right|^2 \qquad (2)$$

where $p_{dif}(\tilde{S}_j,M)$ is obtained as the difference between the total pressure measured at point M and the incident pressure $p_{inc}(\tilde{S}_j,M)$ which is deduced from the known radiation pattern of the reference source $\tilde{S}$.

At the control step the commands U to be sent to the control sources V_k are obtained by minimizing the following expression:

$$\left\| \, p^a_{dif}(S,M) + \sum_{k=1}^{N^C} C_t(V_k,M)\,u(V_k) \, \right\|^2 \qquad (3)$$

where C_t is the transfer matrix between the sources V_k and the point M. The diffracted pressure $p^a_{dif}(S,M)$ is deduced from the estimation of $\widetilde{\mathcal{H}}$ at the previous step:

$$p^a_{dif}(S,M) = \sum_{i=1}^{N^\Gamma} p_{tot}(S,P_i)\,\widetilde{\mathcal{H}}(P_i,M) \qquad (4)$$

where $\widetilde{\mathcal{H}}$ is the solution obtained from Eqn. (2).

3. DESCRIPTION OF THE EXPERIMENT

The experiment is carried out in the semi-anechoic room of the Laboratoire de Mécanique et d'Acoustique (LMA) in which the reflecting wall is vertical, see Fig. 2.

The other five walls are covered with rockwool wedges to ensure a 80 Hz cut-off frequency,excepting the floor which wedges are also covered with a metallic grating which can change their acoustic behavior. For this experiment, the reflecting wall is equipped with control sources and a set of identification microphones is located in a plane parallel to the rigid wall. The source to be characterized and some observation microphones are located in the measurement volume of the semi-anechoic room.

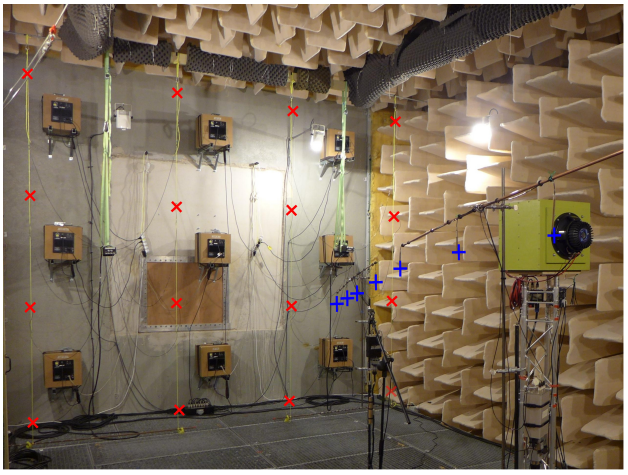

Figure 2. A view of the experiment

Fig. 3 presents a 3D sketch of the experiment, in a (O,x,y,z) rectangular coordinate system. The dimensions, in meter, are $L_x = 9.15$m, $L_y = 4.6$m and $L_z = 4.05$m. The reflecting wall is vertical and corresponds to $x = 0$. The experimental setup features 9 control sources V_k represented by grey squares and fixed on the reflecting wall at a mean distance of $x = 0.15$ m from it and at 3 heights $z = 0.8$m; 2.1m; 3.5m. A rectangular array P_Γ is made of 16 identification microphones represented by red crosses. It is located in a plane parallel to the wall at a distance of 1.2m from it. In order to check the efficiency of the control, 7 observation microphones Q_ℓ represented by blue crosses are located on a line inside the volume Ω. The source S to be characterized is represented by a green circle and located at $x = 5.35$m, $y = 2.98$m, $z = 2.15$m.

Tab. 1 summarizes the distances d_w and d_s : The first one is the distance between the observation microphones Q_ℓ and the surface Γ ; the second one is the distance between observation microphones and the source S.

Microphones	Q_1	Q_4	Q_7
$d_w(\Gamma,Q_\ell)$	1.36	3.25	5.53
$d_s(S,Q_\ell)$	2.77	1.11	1.93

Table 1. Distances in meters d_w and d_s.

In order to estimate the diffraction operator $\mathcal{H}$, the reference source is moved at 32 positions $\tilde{S}_j$ regularly spaced inside a rectangular volume. Their coordinates are given by Table 2.

All measurements are carried out from 40 Hz to 200 Hz, although the cut-off frequency of the anechoic room and

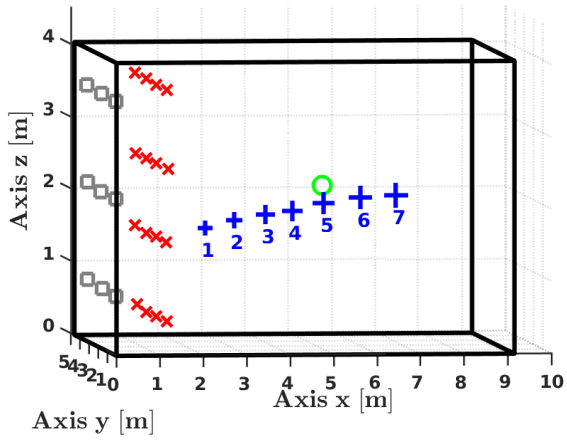

Figure 3. 3D sketch of the experiment - source S (◯), secondary sources V_k (□), identification microphones P_Γ (×), observation microphones Q_{Line} (+)

x	2.14	3.76	5.36	7.0
y	1.2	3.27		
z	1.14	1.64	2.14	2.64

Table 2. Coordinates in meters of the source positions $\tilde{S}_j$

the spatial density of the sensors and actuators imply different lower and upper limits : The classical rule requiring of two samples per wavelength leads to an upper limit of 130 Hz, following the identification microphones spacing, and 110 Hz following the control sources spacing. As a consequence, the frequency range of the active control of the diffracted pressure is expected to be about 80-110 Hz.

4. STRATEGY OF CONTROL : SIMULATIONS

Numerical simulations were conducted using a custom software (named FELIN) based on the Boundary Element Method (BEM). The configuration used for the numerical simulations corresponds to the geometry of the room used for the experiment. The computations were carried out in the 40-200 Hz frequency band. Therefore the maximum dimension of the room is of the order of 5.4 wavelengths. For the sake of simplicity, the acoustic behaviour of the walls is described by a localised boundary condition (reduced normal admittance β). The reflecting wall is described by a small admittance value $\beta = 10^{-3} + i\ 10^{-3}$ and the absorbing walls by $\beta = 1 + i\ 0$. These values are uniform on each wall and kept constant over the whole frequency band. In the simulations, all sources are assumed to be ideal monopole sources with prescribed volume velocity. Their positions are supposed to represent the acoustic centres of the actual sources used for the experiment.

Fig. 4 represents the geometry for the simulation. The set M_Ω includes 54 control microphones M_ℓ located in Ω ; they are used to compute the commands for the active control. They are equally spaced inside a rectangular volume defined by $3\text{m} \leq x \leq 6\text{m}; 2\text{m} \leq y \leq 3\text{m}; 1.5\text{m} \leq z \leq 2.8\text{m}$. The sets Q_{Line} and Q_{Plane} correspond to observation microphones inside Ω, used to check the efficiency of the control. The 119 points of Q_{Plane} are equally spaced in a plane horizontal array defined by $1.8\text{m} \leq x \leq 7.2\text{m}; 1.2\text{m} \leq y \leq 3.3\text{m}; z = 1.8\text{m}$.

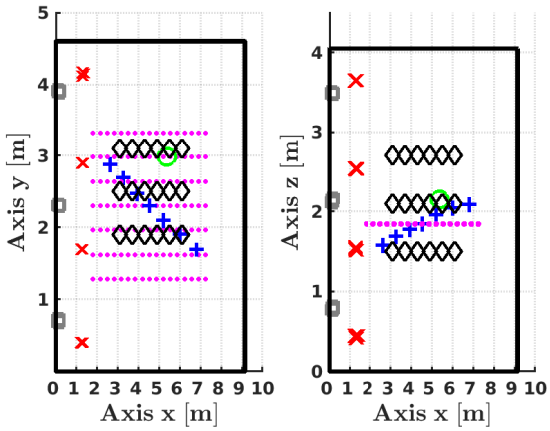

Figure 4. Geometry for simulations - source S (◯), secondary sources V_k (□), identification microphones P_Γ (×), control microphones M_Ω (◊), observation microphones Q_{Plane} (•), observation microphones Q_{Line} (+)

4.1 Control on M_Ω with the exact diffracted pressure

Now, the control is used to minimize the exact diffracted pressure over the M_Ω set. The resulting pressures are observed on the Q_{Line} and Q_{Plane} sets.

Fig. 5 and Fig. 6 present levels (in dB) obtained at 95 and 125 Hz with control off and on respectively. At each point, the levels represent the difference between the total pressure and the incident pressure, for the point source $\tilde{S}$. The coloured lines map the results on Q_{Plane}. The coloured diamonds numbered from 1 to 7 correspond to Q_{Line} superimposed over the map, although they are not in the Q_{Plane} plane. On the left-hand side of each map, the vertical line of the four diamonds indicates the level computed at each identification microphones P_Γ. Each diamond divided into 4 parts corresponds to a vertical line of 4 microphones. Green levels (between ± 1.5 dB) mean that the diffracted pressure is small or efficiently controlled. When control is off, the map points out the effect of the boundaries. Especially, significant differences between the incident and total pressures can be seen close to the reflecting wall. These differences are observed over a large part of the measuring area, especially at 125 Hz.

When control is on, most of the observation points belong to a green area. The best results are obtained at 125 Hz for which the control is quite efficient for all abscissas larger than 2.3 m. These results show that control on M_Ω does lead to correct results on Q_{Line} and Q_{Plane} although Q_{Plane} extends outside the boundaries of M_Ω. Exception

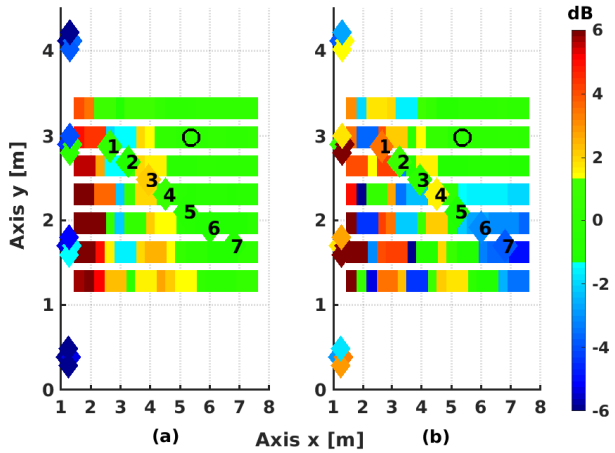

Figure 5. Level without control observed on Q_{Line} and Q_{Plane} at - (a) 95 Hz, (b) 125 Hz

must be noticed for the area close to the reflecting wall where the difference in levels goes above 6 dB.

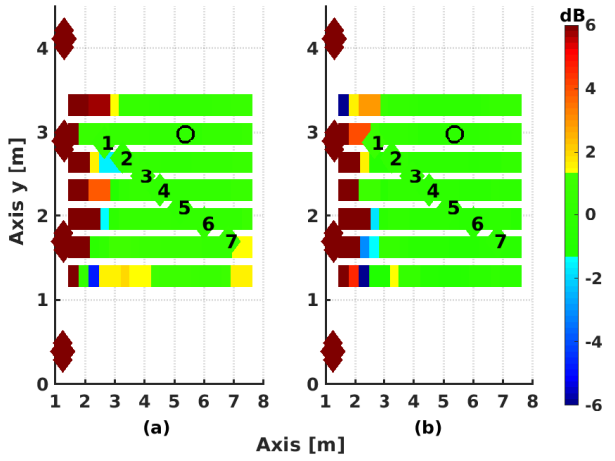

Figure 6. Control on M_Ω observed on Q_{Line} and Q_{Plane} at - (a) 95 Hz, (b) 125 Hz

A global diffraction control in Ω seems thus achievable, but it requires a large number of control microphones within the measuring volume. More simulations using a lower number of microphones showed that this number may indeed be reduced but satisfying performances anyway requires a repartition of microphones inside Ω, which is not suitable in practice.

4.2 Control on P_Γ with the exact diffracted pressure

Here the P_Γ set is also used as control microphones.

Fig. 7 shows that the control on P_Γ is almost as efficient as the control on M_Ω. The diffracted pressure is reduced even at locations far from Γ. At these frequencies, the density of microphones seems to be sufficient, which is consistent with a minimum spacing of a half-wavelength. Furthermore the increase of the pressure in the vicinity of the reflective wall is smaller than in Fig. 6.

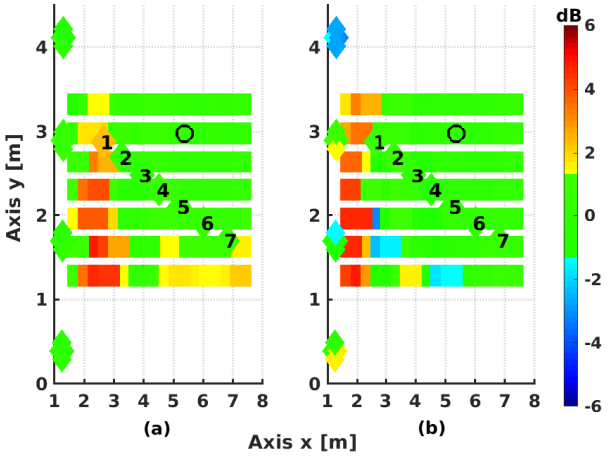

Figure 7. Control on P_Γ observed on Q_{Line} and Q_{Plane} at - (a) 95 Hz, (b) 125 Hz

More simulations presented in [12, 17] show that the results of control obtained with the estimated diffracted pressure are quite similar to those obtained with the exact diffracted pressure. They show that the estimation of the diffraction operator does not require a high accuracy, at least as far as the radiation pattern of the reference source is correctly described. This is an encouraging preliminary result as it would validate the control of diffraction using a single layer of pressure measurements on Γ.

The aim here was to carry out a first full-scale experiment in order to assess the efficiency of the control in a realistic situation. The previous simulations validate the configuration minimizing the diffracted pressure over the same set P_Γ as the one used to estimate the diffraction operator $\mathcal{H}$. This is a good point as such a configuration leads to a relatively simple experimental set-up.

5. EXPERIMENTAL RESULTS

The experiment is based on two sets of microphones, that is P_Γ for both identification and control steps and Q_{Line} used to check the efficiency of the control. The corresponding geometry is presented in Fig. 3.

This experiment is based on the use of a low-frequency omnidirectional compact source. It was designed and made at LMA and equipped with an internal microphone in order to estimate the flow inside the source. This source is assumed to be a sphere which radius is small compared to the distance r between the source and the measurement point. With the time dependency $\mathrm{e}^{\imath\omega t}$, the acoustic pressure in free field at a point M can be written as:

$$p_{inc}(S,M) = \frac{\imath\omega\rho_0 Q_s}{4\pi}\,\frac{\mathrm{e}^{-\imath kr(S,M)}}{r(S,M)} \qquad (5)$$

where Q_s is the flow, ω the angular frequency, k the wave number and ρ_0 the density of the air. The details of the source model are described in [12, 18].

For practical reasons, the same source was used at the $\tilde{S}_j$ set of positions for the identification step, in order to identify the filter matrix $\mathbf{H}$, and then used again as the "unknown" source S to be characterized. The matrix $\mathbf{H}$ defined by

$$\mathbf{H}_{k\ell} = \mathcal{H}(P_k, P_\ell) \text{ for k and } \ell = 1, \ldots, N^\Gamma$$

is obtained by minimizing Eqn. (2) with $F(\tilde{S}_j, P_i)$ for $j = 1$ to N^H and $i = 1$ to N^Γ

5.1 Method

The experiment of the active control of the diffracted field on the surface Γ is split into 2 steps. The identification step requires the following terms: $p_{tot}(\tilde{S}_j, P_i)$ and $p_{dif}(\tilde{S}_j, P_i)$; $N^H = 32$ positions $\tilde{S}_j$ were used in order to improve the process. The total pressures were directly measured. The second ones were deduced as the difference between the total pressure and the incident pressure $p_{inc}(\tilde{S}_j, P_i)$ which was estimated from the measurement of the reference pressure at the microphone located inside the source, following Eqn. (5).

For the control step, all transfer functions $C_t(V_k, P_i)$ were first measured. Then the total pressures $p_{tot}(S, P_i)$ were measured in order to compute the diffracted pressures (to be minimized) $p^a_{dif}(S, P_i)$ obtained from Eqn. (4). Finally the source commands $u(V_k)$ were obtained by minimizing the cost function at the locations P_Γ, following Eqn. (3).

The pressure radiated by the S source was measured at all microphones with the active control off and on. A sine sweep signal was used at the identification step and for the measurement of the transfer functions $C_t(V_k, P_i)$ and $C_t(V_k, Q_\ell)$. During the control step, the commands were then calculated, for several frequencies, according to Eqn. (3). At each frequency, the measurements with active control were carried out in real-time, the signals of the reference and control sources were sine signals. In addition, an estimation of the control at each Q_ℓ was computed by combining measurement and computation according to the following equation :

$$p^e_{on}(S, Q_\ell) = p_{tot}(S, Q_\ell) + \sum_{k=1}^{9} C_t(V_k, Q_\ell) u(V_k) \quad (6)$$

where p_{tot} is the total pressure measured without control and the elements $C_t(V_k, Q_\ell)$ correspond to the measured transfer functions between V_k and Q_ℓ.

5.2 Results

The measurement results are presented with control off and on. They are plotted as levels function of frequency, in a way similar to the one recommended by the ISO 3745 standard. All pressures are normalized by the incident pressure p_{inc} estimated following Eqn. (5) so that 0 dB represents the fully anechoic case. The black dashed horizontal lines at ± 1.5 dB indicate the lower and upper limits for acceptance of an anechoic room at low frequencies. The dotted red curve represents the total pressure p_{off} measured without control. The diamond symbol represents, at several frequencies, the total pressure p_{on} measured in real-time with control and the black curve represents the estimation of the control p^e_{on} given by Eqn. (6).

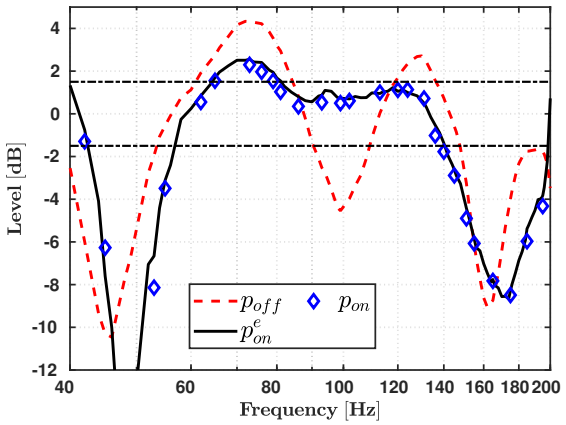

Figure 8. Observation microphone Q_1

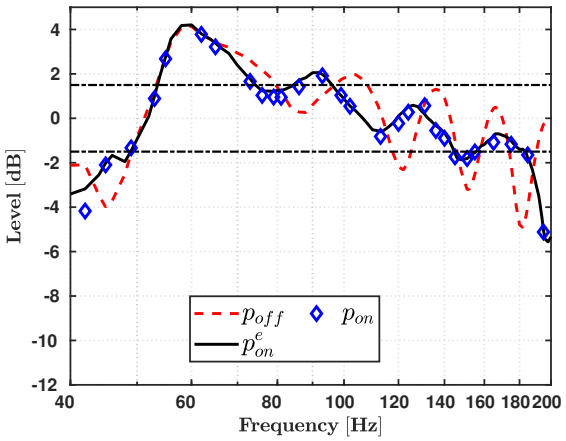

Figure 9. Observation microphone Q_7

Fig. 8 and Fig. 9 respectively present the results at the observation microphones Q_1 (close to the reflecting wall) and Q_7 (far from the reflecting wall). The measurements with control off p_{off} point out the frequency fluctuations resulting from the interferences between the source S and the image source. The measurements carried out with control on show a significant attenuation of the diffracted field in the frequency band $[80 - 140]$ Hz for Q_1. For Q_7, the level is inside the interval ± 1.5 dB between 80 to 180 Hz with two exceptions around 90 and 140 Hz. As expected, the control has almost no effect below about 75 Hz : Below the room cut-off frequency, significant reflections occur on all walls and the room response is dominated by acoustic modes. Reducing the diffraction of a single wall can barely

have a large effect when the contribution of the other walls is significant.

These satisfactory results indicate on the one hand that the diffraction operator has been well estimated and on the other hand that the control of the diffracted pressure on the surface does lead to an attenuation in the volume as seen with the simulation (Fig. 7). The limits of control efficiency could correspond to the limits imposed by the constraints of the experiment seen in section Sec. 3. Moreover, the estimated control gives similar results than those directly measured. This consistency is interesting and allows to consider testing different control parameters.

Let us finally point out that a decrease of the levels can be observed above 120 Hz. In this case, the model of the source $\tilde{S}$ used was a monopole source. This point is discussed in details in [18] and [17] where it is shown that a more accurate model of the source radiation is indeed necessary.

6. CONCLUSION

The simulations and experimental results obtained for the control in the semi-anechoic room show that the control strategy on the surface Γ is efficient. It seems that the estimation of the diffracted pressure does not require a high accuracy for the operator $\mathcal{H}$ but does require an accurate model of the reference source. However these first results have to be backed by more extensive simulations and experimentations for assessing the influence of all parameters involved.

7. REFERENCES

[1] M. Furstoss, D. Thenail, and M.-A. Galland, "Surface impedance control for sound absorption : Direct and hybrid passive-active strategies," *J. Sound Vib.*, vol. 203, no. 2, p. 219–236, 1997.

[2] H. Lissek, R. Boulandet, and R. Fleury, "Electroacoustic absorbers: Bridging the gap between shunt loudspeakers and active sound absorption," *The Journal of the Acoustical Society of America*, vol. 129, no. 5, pp. 2968–2978, 2011.

[3] B. Betgen and M.-A. Galland, "A new hybrid active/passive sound absorber with variable surface impedance," *Mech. Syst. Sig. Proc.*, vol. 25, no. 5, pp. 1715–1726, 2011.

[4] M. Melon, C. Langrenne, D. Rousseau, and P. Herzog, "Comparison of four subwoofer measurement techniques," *J. Audio Eng. Soc.*, vol. 55, no. 12, pp. 1077–1091, 2007.

[5] M. Melon, C. Langrenne, and P. Herzog, "Evaluation of a method for the measurement of subwoofers in usual rooms," *J. Acoust. Soc. Am.*, vol. 127, no. 1, pp. 256–263, 2010.

[6] M. Sanalatii, P. Herzog, R. Guillermin, M. Melon, N. Poulain, and J.-C. Le Roux, "Estimation of loudspeaker frequency response and directivity using the radiation-mode method," *J. Audio Eng. Soc.*, vol. 67, no. 3, pp. 101–115, 2019.

[7] AFNOR, *Norme ISO 3745, Acoustique - Détermination des niveaux de puissance acoustique émis par les sources de bruit à partir de la pression acoustique - Méthodes de laboratoire pour les salles anéchoïques et semi-anéchoïques*, 2013.

[8] E. Friot and A. Gintz, "Estimation and global control of noise reflections," in *Active 2009*, (Ottawa, Canada), 2009.

[9] P. Herzog, E. Friot, D. Habault, C. Pinhède, A. Gintz, P. Leroy, and M. Pachebat, "Toward an active anechoic room," in *7th Forum Acusticum*, no. R01-3, (Krakow, Poland), European Acoustical Association, 2014.

[10] D. Habault, E. Friot, P. Herzog, and C. Pinhède, "Active control in an anechoic room : Theory and first simulations," *Acta Acustica united with Acustica*, vol. 103, no. 3, pp. 369–378, 2017.

[11] C. Pinhède, D. Habault, P. Herzog, and E. Friot, "Contrôle actif du champ diffracté en basse fréquence dans une salle semi-anéchoïque," in *Proc. Congrès Français d'Acoustique*, (Le Havre, France), 2018.

[12] C. Pinhède, *Contrôle actif aux basses fréquences du champ diffracté en salle semi-anéchoïque*. PhD thesis, Aix-Marseille Université, 2019.

[13] E. Friot and C. Bordier, "Real-time active suppression of scattered acoustic radiation," *Journal of Sound and Vibration*, vol. 278, no. 3, pp. 563–580, 2004.

[14] E. Friot, R. Guillermin, and M. Winninger, "Active control of scattered acoustic radiation: a real-time implementation for a three-dimensional object," *Acta acustica united with acustica*, vol. 92, pp. 278–288, 2006.

[15] A. Gintz, *Estimation des échos à basse fréquence dans un local de mesure*. PhD thesis, Aix-Marseille 1, 2009.

[16] P. Leroy, "Rapport final du post-doctorat sur l'estimation du champ diffracté dans la maquette de chambre sourde active," tech. rep., 2010.

[17] C. Pinhède, D. Habault, P. Herzog, and E. Friot, "Active control of reflections in a semi-anechoic room - simulations and a full-scale off-line experiment," *Journal of Sound and Vibration*, 2020 - submitted.

[18] C. Pinhède and P. Herzog, "Design and measurement of a reference source at lower frequencies," in *Proc. Forum Acusticum*, 2020.